

Available online at www.sciencedirect.com



Trans. Nonferrous Met. Soc. China 21(2011) 801-806

Transactions of Nonferrous Metals Society of China

www.tnmsc.cn

# Microstructure of 18R-type long period ordered structure phase in Mg<sub>97</sub>Y<sub>2</sub>Zn<sub>1</sub> alloy

TANG Ping-ying<sup>1</sup>, WU Meng-meng<sup>1</sup>, TANG Bi-yu<sup>1, 2</sup>, WANG Ji-wei<sup>2</sup>, PENG Li-ming<sup>3</sup>, DING Wen-jiang<sup>3</sup>

- 1. School of Chemistry and Chemical Engineering, Guangxi University, Nanning 530004, China;
- 2. Faculty of Materials, Optoelectronics and Physics, Xiangtan University, Xiangtan 411105, China;
- Light Alloy Net Forming National Engineering Research Center, School of Materials Science and Engineering, Shanghai Jiao Tong University, Shanghai 200030, China

Received 25 September 2010; accepted 20 December 2010

**Abstract:** The microstructure of the 18R-type long period stacking ordered (LPSO) phase in  $Mg_{97}Y_2Zn_1$  alloy was investigated by the first principles calculation. The arrangement rule of Zn and Y atoms in the LPSO structure is determined theoretically. The calculation results reveal that the additive atoms are firstly located in the fault layers at the two ends of the 18R-type LPSO structure, and then extend to fault layers in the interior, which is in good agreement with the experimental observations. This feature also implies the microstructural relationship between 18R and other LPSO structures. The cohesive energy and the formation heat indicate the dependence of the stability of 18R LPSO structure on contents of Y and Zn atoms. The calculated electronic structures reveal the underlying mechanism of microstructure and the stability of 18R LPSO structure.

Key words: Mg<sub>97</sub>Y<sub>2</sub>Zn<sub>1</sub> alloy; 18R LPSO structure; the first principles; microstructure; electronic structure

## 1 Introduction

Great importance has been attached to Mg-based alloys, because of its low density, high specific strength and specific elastic modulus, exceptional dimensional stability, high damping capacity, and high recycling efficiency[1]. Mg-based alloys with superior properties have been applied in many areas such as microelectronics, automobile and aerospace industries. However, the lower tensile strength and inferior ductility of Mg-based alloys still limit its wide applications.

Much effort has been devoted to further improving the mechanical property. Recently, the Mg<sub>97</sub>Y<sub>2</sub>Zn<sub>1</sub>(mole fraction, %) alloy with a yield strength of 610 MPa and elongation of 5% was developed by rapidly solidified powder metallurgy (RS P/M) processing, and it also exhibited high corrosion resistance at room temperature [2–3]. These excellent properties are considered to be due to the hcp (2H)-Mg fine grain matrix of 100–200 nm in diameter, a novel long-period stacking ordered (LPSO)

phase and homogeneously dispersed Mg24Y5 fine particles[4-6]. Since LUO et al[7-8] identified the X-phase in Mg-Y-Zn cast alloy as an 18R-tpye LPSO structure, many investigations have been focused on the novel LPSO phases. Up to now, five kinds of LPSO structures (6H, 10H, 14H, 18R, and 24R) have been observed experimentally[8-14]. Furthermore, two kinds of 18R-type LPSO structures have been reported with electron diffraction experiments[12–13]. ABABABCACACABCBCBC with the lattice constants of a=3.20 Å and c=46.78 Å, the other ACBCBCBACACACBABAB with the lattice constants of a=3.20 Å and c=48.6 Å. On the other hand, the inter-transformation is also observed among different LPSO structures. Experimental investigations revealed that the 18R LPSO structure ACBCBCBACACACBA-BAB was transformed to 14H LPSO structure ABABABACBCBCBC in the cast Mg-Zn-Y alloys during heat treatment[13], and the 14H LPSO structure ABABABACACACAC was found to change into a six-layered atomic array structure ABACAB by

Foundation item: Projects (50861002, 51071053) supported by the National Natural Science Foundation of China; Project (0991051) supported by Natural Science Foundation of Guangxi Province, China; Project (KF0803) supported by Open Project of Key Laboratory of Materials Design and Preparation Technology of Hunan Province, China; Project (X071117) supported by Scientific Research Foundation of Guangxi University, China

Corresponding author: TANG Bi-yu; Tel: +86-731-58292195; E-mail: tangbiyu@xtu.edu.cn DOI: 10.1016/S1003-6326(11)60784-X

annealing [14].

The novel LPSO structures have also been found experimentally in other Mg-RE-Zn, Mg-Cu-RE and Mg-TM-Zn alloys[15–19]. It can be predicted that various LPSO phases would be found in many Mg-TM-RE alloys, so the investigations of the microstructure and formation are necessary and important. However, the theoretical study of LPSO structures in such Mg-RE-Zn alloys is very scarce. In the present work, the accurate positions and arrangement rule of Zn and Y atoms were firstly determined theoretically, and then the space distributions of the Y and Zn atoms in 18R-type LPSO structure of ACBCBCBACACACBABAB were studied. inter-transformation among different LPSO structures and the stability of various LPSO structures were also discussed.

#### 2 Calculation method

The present calculations were performed using the Vienna Ab initio Simulation Package (VASP)[20-21]. The exchange-correlation functional was described within the generalized gradient approximation (GGA) of Perdew-Burke-Ernzerhof (PBE)[22], and the projector augmented wave method[21-22] was used for description of the ion-valence electron interaction, and the kinetic energy cutoff was chosen to be 300 eV. The valence electron configurations considered were 3s, 2p for Mg, 3d, 4s for Zn and 4s, 4p, 5s, 4d for Y. The Brillouin zone was sampled with a mesh of  $5 \times 3 \times 1$ k-points of Monkhorst-Pack scheme[23] for the supercell (2×3×18) 18R-tpye LPSO. These parameters were tested to be sufficient for convergence. Structural optimization was firstly performed using the first-order Methfessel-Paxton method with a temperature broadening parameter of 0.2 eV, and the positions of atoms were fully relaxed until the total forces on each ion were less than 0.03 eV/Å. Then the total energy was calculated using the tetrahedron method with the Blöchl corrections[24].

#### 3 Results and discussion

#### 3.1 Microstructure

In order to test the parameters and pseudopotentials, lattice constants of the 2H pure Mg were calculated. The obtained results were a = 3.19 Å and c = 5.20 Å for 2H pure Mg, which were in good agreement with the experimental values[14] and other theoretical calculations[25].

To simulate the configuration of 18R-type LPSO structure in  $Mg_{97}Y_2Zn_1$  alloy, we adopted a  $2\times3\times18$  supercell with 108 atoms. Figure 1 shows the two-dimensional lattice in the base plane of the structural unit.

If only one Zn or Y atom is added, the present calculation results show that the single Zn or Y atom would occupy any position in the fault layer A at the end of the LPSO structure, which is similar to our previous investigation for 6H LPSO structure[26-27]. For convenient of description, it is assumed that the single Zn or Y atom occupies the origin of layer A in the unit cell, labeled by point 1 in Fig.1. In terms of the present calculation results shown in Table 1, if one Zn and one Y atoms are simultaneously added, the additive Zn and Y atoms would locate in positions 1 and 4 in the layer A, respectively. The calculation results in Table 2 show that when one Zn and two Y allovs are added, if the first Zn atom occupies the origin of layer A, the other two Y atoms will locate in the points 4 and 6. If the alloys simultaneously contain two Zn atoms and two Y atoms, Zn atoms will take up positions 1 and 3 while Y atoms occupy points 4 and 6. With further addition of Zn or Y atom, the following Zn or Y atom will diffuse to other atomic layer, indicating that the atomic number for substitution saturation of the bottom layer A of 18R LPSO structure is approximately 4. Moreover, when the contents of Zn and Y atoms in the bottom layer A reach saturation, the atomic arrangement forms two parallel lines, the left one is Zn atoms, while the right one is the Y atoms.

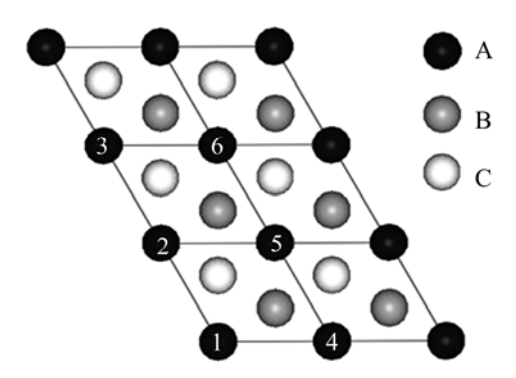


**Fig.1** Atomic arrangement model of 18R-type LPSO structure (The model is 2×3 unit cell, and A, B and C represent the layers of A, B and C, respectively)

**Table 1** Distribution of 1Zn+1Y atoms in bottom layer (Points 1–6 correspond to number in Fig.1)

	Total						
1	2	3	4	5	6	energy/eV	
1Zn	1Y					-168.832 40	
1Zn		1Y				-168.832 39	
1Zn			1Y			-168.863 19	
1Zn				1Y		-168.817 45	
1Zn					1Y	-168.818 69	

**Table 2** Distribution of 1Zn+2Y and 2Zn+1Y atoms in bottom layer (Points 1–6 correspond to number in Fig.1)

	Total					
1	2	3 4		5	6	energy/eV
1Zn	1Y		1Y			-173.519 27
1Zn		1Y	1Y			-173.387 39
1Zn			1Y	1Y		-173.368 45
1Zn			1Y		1Y	-173.654 38
1Zn	1Zn		1Y		1Y	-173.547 93
1Zn		1Zn	1Y		1Y	-173. 653 84
1Zn			1Y	1Zn	1Y	-173.594 72

The microstructure of the bottom layer A for 18R LPSO structure is different from that of 6H LPSO structure due to the difference of the two-dimensional unit cell (4×4 and 2×3 for 6H and 18R LPSO structure, respectively). For 18R LPSO structure, before the saturation of substitution atom in the bottom of layer A, two Zn atoms will simultaneously locate in the single layer A. For 6H LPSO structure, two Zn atoms will diffuse into two different atomic layers[26–27].

When more atoms x Zn and y Y  $(5 \le x + y \le 8, 3 \le x \le 4)$ , are added in the 18R-type LPSO phase, the additive atoms Zn and Y will not be restrained to a single layer but diffuse to another one. The following additives will locate in the second layer C, corresponding to the other end of the LPSO structure. Similar to the arrangement in the layer A, the third additional Zn atom would take up the point 1 in the layer C, while following more Y atoms will locate in points 4 and 6 in layer C. Therefore, the present calculations show that with eventual addition of Zn and Y atoms, the additive atoms will be significantly enriched at both the bottom layer A and the second layer C in the 18R LPSO structure. This arrangement of additive atoms on the fault layers at the two ends of the LPSO structure is in good agreement with the experimental observations[15, 28-29], and is also similar to our previous investigation for 6H LPSO

structure[26–27]. The arrangement in the second layer C will be also along two diagonal lines. Furthermore, the diagonal line in the second layer C is parallel to the diagonal line in the layer A.

Experiments also show that most Zn and Y atoms locate in stacking fault layers at the two ends of the LPSO phase, a small amount of additives are distributed in the interior LPSO phase[6]. The distribution position and mechanism are still not clarified. In order to clearly investigate the small amount of additives in the interior LPSO structure, more Zn and Y atoms are added. The calculation results in Table 3 reveal that the following Zn atoms will take up the point 6 of the 8th layer in the 18R LPSO structure, while the following two atoms of Y will occupy point 3 in the 8th layer and point 6 in the 14th layer of the 18R LPSO structure. The overall space distribution feature of the additive atoms indicates that, most Zn and Y are mainly enriched in the stacking fault layers the ends ACtwo ACBCBCBACACACBABAB structure, then a small amount of the additive atoms Zn and Y are distributed at the three stacking fault layers AC, BA and CB in the interior of LPSO phase. The present results are well consistent with the experimental observations[6, 28–29].

It has been reported that various LPSO structures could be inter-transformed from one type into others[13-14]. From the calculation results shown in Table 3, it is found that the additive elements of Zn and Y in the 8th layer implied inter-transformation tendency among 18R and other LPSO structures. Because Zn and Y atoms are distributed in the fault layers AC, BA and CB of the 18R-tpye LPSO ACBCBCBACACACBABAB stacking sequence, when their contents reach definite values, the 18R-tpye LPSO may break from the fault layer, forming the stacking sequences of ACBCBC and BACACACBABAB or the stacking sequences of **CBABAB** ACACABCBCBCA. Further study on the microscopic details of the inter-transformation is under way.

Table 3 Element distribution at relatively high concentrations in long-period ordered structure

Layer							Total		
A	С	BCBC	В	A	CACA	C	В	ABAB	energy/eV
2Zn+2Y									-173.460 46
2Zn+2Y	2Y								-184.551 69
2Zn+2Y	1Zn+2Y								-184.332 05
2Zn+2Y	1Zn+2Y		1Y						-189.339 00
2Zn+2Y	1Zn+2Y		1Y			1Y			-194.354 54
2Zn+2Y	1Zn+2Y		1Y			1Y	1Y		-199.417 23
2Zn+2Y	2Zn+2Y		1Y			1Y	1Y		-199.238 57
2Zn+2Y	2Zn+2Y		1Y	1Zn		1 <b>Y</b>	1Y		-199.197 51
2Zn+2Y	1Zn+2Y		1Y	1Y+Zn		1Y	1Y		-204.104 57

#### 3.2 Formation heat and cohesive energy

In order to assess structural stability of alloys[30], the average formation heat of the 18R-tpye LPSO structures per atom can be calculated by[31]

$$\Delta H = \frac{1}{x + y + z} (E_{\text{tot}} - x E_{\text{solid}}^{\text{Mg}} - y E_{\text{solid}}^{\text{Y}} - z E_{\text{solid}}^{\text{Zn}})$$
 (1)

where  $E_{\rm tot}$  is the total electronic energy of unit cell;  $E_{\rm solid}^{\rm Mg}$ ,  $E_{\rm solid}^{\rm Y}$ , and  $E_{\rm solid}^{\rm Zn}$  are the total energies of single Mg, Y and Zn atom in their pure solid states, and the calculated values are -1.517 3, -6.381 1 and -1.109 8 eV for Mg, Y and Zn, respectively; x, y and z are the numbers of Mg, Y and Zn atoms, respectively, in unit cell. The average formation heats of 18R-type LPSO for various compositions are displayed visually in Fig.2. It is clearly shown that the stability of the 18R LPSO phases is better with addition of Y.

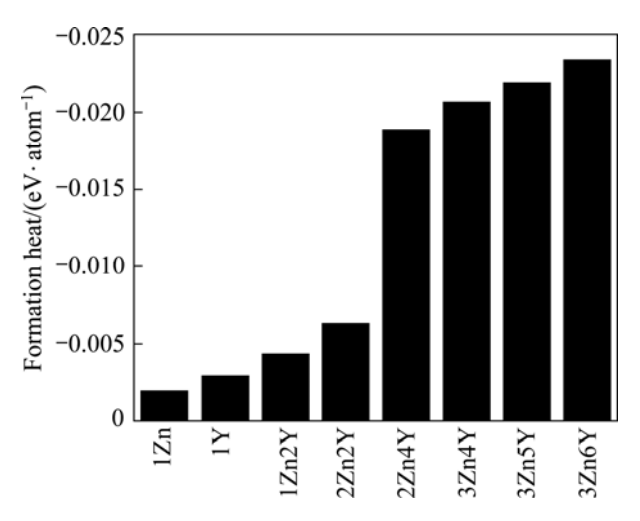


Fig.2 Formation heats of 18R-type LPSO phase

The stability of crystal structure is also correlated to its cohesive energy[32], and the cohesive energy is often defined as energy needed when crystal is decomposed into the single atom. Hence, the lower the cohesive energy is, the more stable the crystal structure is[32]. In this work, average cohesive energy per atom for the 18R-tpye LPSO structures was calculated using the following expression[31]:

$$E_{\rm coh} = \frac{1}{x + y + z} (E_{\rm tot} - xE_{\rm atom}^{\rm Mg} - yE_{\rm atom}^{\rm Y} - zE_{\rm atom}^{\rm Zn})$$
 (2)

where  $E_{\rm atom}^{\rm Mg}$ ,  $E_{\rm atom}^{\rm Y}$  and  $E_{\rm atom}^{\rm Zn}$  are the total electronic energies of single Mg, Y and Zn atoms in freedom states, and they are -0.0398, -1.987 0 and -0.005 5 eV for Mg, Y and Zn free atoms, respectively. The obtained cohesive energies are displayed in Fig.3. It can be clearly found that the average cohesive energy of 18R-type is negative, hence 18R-type LPSO structures are stable. It is interesting that with addition of Zn atoms, the cohesive

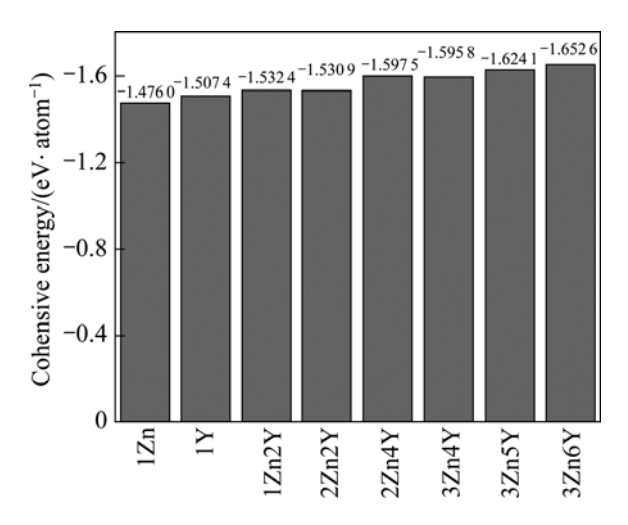


Fig.3 Cohesive energies of 18R-type LPSO phase

energy is increased slightly. From the above calculation results of formation heats and cohesive energies, it could be expected that the 18R-type crystal is stable.

#### 3.3 Electronic structure

In order to further understand the structural feature of 18R LPSO phase in the Mg<sub>97</sub>Y<sub>2</sub>Zn<sub>1</sub>, the charge densities are calculated, as displayed in Fig.4. The higher charge density region corresponds to the core electron distribution of Y, Zn and Mg atoms, which contributes relatively little to the bonding. It can be seen from Figs.4 (a) and (b) that the obvious overlap of the charge densities occurs among Mg-Mg, Mg-Y and Mg-Zn, indicating that the covalent bonding is formed among those atoms. From the electronic structure, a maximum is observed in the center of the tetrahedral electronic network, corresponding to the midpoints between Mg-Mg atoms. The charge distribution displayed in Figs.4 (c) and (d) also shows that maxima between Mg-Y and Mg-Zn atoms becomes weaker. In contrast to the Mg-Mg bonding, there is no overlap of electron densities between Y-Y and Zn-Zn atoms. The electron structure exhibits a metallic bonding between Y-Y and Zn-Zn, and can be described by the nearly free electron model.

### 4 Conclusions

1) The additive Y and Zn atoms are firstly mainly concentrated in the stacking fault layers at the two ends of the 18R-type LPSO phase, and then a small amount of additional atoms disperse into the stacking faults <u>BA</u> and <u>CB</u> in the interior of the LPSO structure, which is in good agreement with the reported experimental observation. This distribution feature implies the inter-transformation tendency among 18R-type and other type LPSO structure.

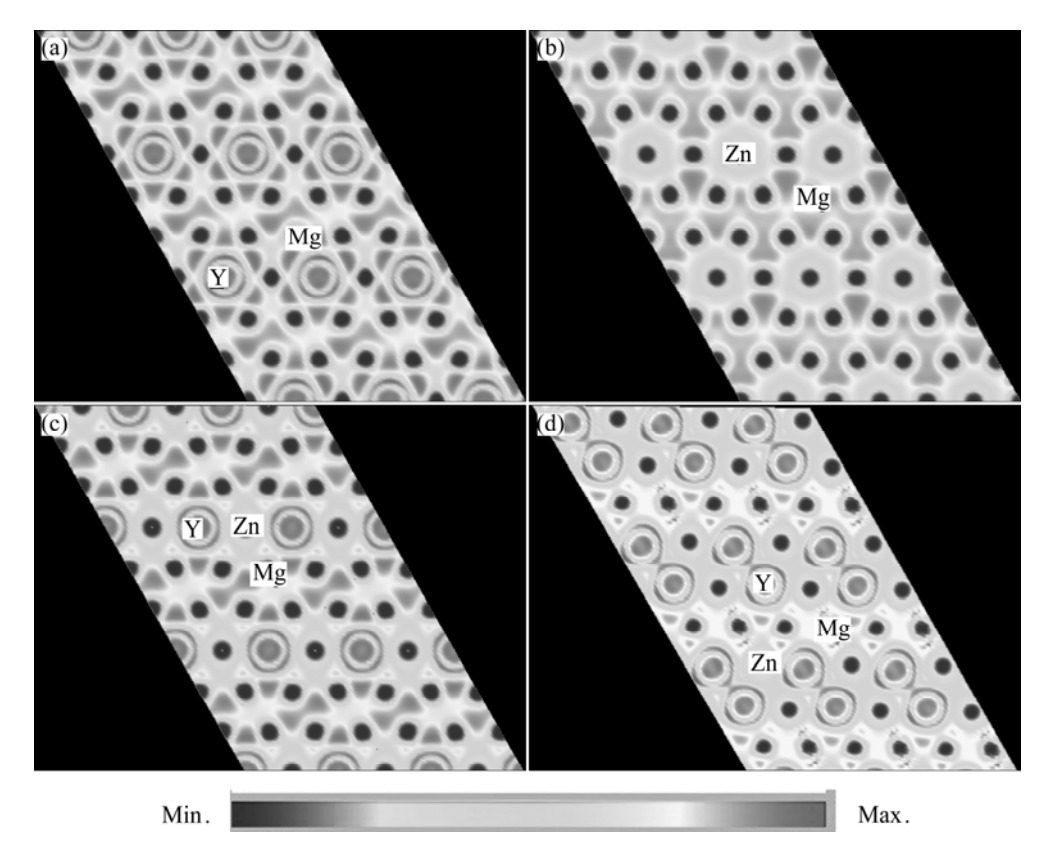


Fig.4 Charge densities of 18R-type LPSO phase containing 1Y (a), 1Zn (b), 1Zn1Y (c) and 3Zn6Y (d)

- 2) The calculation results of cohesive energy and formation heat show that 18R-type LPSO structure is stable from the energetic point of view.
- 3) The calculated electronic structures demonstrate that the covalent bonding is formed among Mg-Mg, Mg-Y and Mg-Zn atoms, so the 18R LPSO structure possesses higher stability and strength.

#### References

- EDGAR R L. Magnesium alloys and their application [M]. France: Kainer K U, 2003: 3-4.
- [2] KAWAMURA Y, HAYASHI K, INOUE A, MASUMOTO T. Rapidly solidified powder metallurgy Mg<sub>97</sub>Zn<sub>1</sub>Y<sub>2</sub> alloys with excellent tensile yield strength above 600 MPa [J]. Materials Transactions, 2001, 42: 1172–1176.
- [3] YAMASAKI M, NYU K, KAWAMURA Y. Corrosion behavior of rapidly solidified Mg-Zn-Y alloy ribbons [J]. Materials Science Forum, 2003, 419–422: 937–942.
- [4] NISHIDA M, YAMAMURO T, NAGANO M, MORIZONO Y, KAWAMURA Y. Electron microscopy study of microstructure modifications in RS P/M Mg<sub>97</sub>Zn<sub>1</sub>Y<sub>2</sub> alloy [J]. Materials Science Forum, 2003, 419–422: 715–720.
- [5] ABE E, KAWAMURA Y, HAYASHI K, INOUE A. Long-period ordered structure in a high-strength nanocrystalline Mg-1at% Zn-2at% Y alloy studied by atomic-resolution Z-contrast STEM [J]. Acta Materialia, 2002, 50: 3845–3857.
- [6] PING D H, HONO K, KAWAMURA Y, INOUE A. Local chemistry of a nanocrystalline high-strength Mg<sub>97</sub>Y<sub>2</sub>Zn<sub>1</sub> alloy [J]. Philosophical Magazine Letters, 2002, 82: 543–551.

- [7] LUO Z P, ZHANG S Q. High-resolution electron microscopy on the X-Mg12ZnY phase in a high strength Mg-Zn-Zr-Y magnesium alloy [J]. Journal of Materials Science Letters, 2000, 19: 813–815.
- [8] LUO Z P, ZHANG S Q, TANG Y L, ZHAO D S. Microstructures of Mg-Zn-Zr-RE alloys with high RE and low ZN contents [J]. Journal of Alloys and Compounds, 1994, 209: 275–278.
- [9] POLMEAR I J. Magnesium alloys and applications [J]. Materials Science and Technology, 1994, 10: 1–16.
- [10] KAWAMURA Y, KASAHARA T, IZUMI S, YAMASAKI M. Elevated temperature Mg<sub>97</sub>Y<sub>2</sub>Cu<sub>1</sub> alloy with long period ordered structure [J]. Scripta Materialia, 2006, 55: 453–456.
- [11] MATSUDA M, LI S, KAWAMURA Y, IKUHARA Y, NISHIDA M. Interaction between long period stacking order phase and deformation twin in rapidly solidified Mg<sub>97</sub>Zn<sub>1</sub>Y<sub>2</sub> alloy [J]. Materials Science and Engineering A, 2004, 386: 447–452.
- [12] MATSUDA M, LI S, KAWANURA Y, IKUHARA Y, NISHIDA M. Variation of long-period stacking order structures in rapidly solidified Mg<sub>97</sub>Zn<sub>1</sub>Y<sub>2</sub> alloy [J]. Materials Science and Engineering A, 2005, 393: 269–274.
- [13] ITOI T, SEIMIYA T, KAWAMURA Y, HIROHASHI M. Long period stacking structures observed in Mg<sub>97</sub>Zn<sub>1</sub>Y<sub>2</sub> alloy [J]. Scripta Materialia, 2004, 51: 107–111.
- [14] AMIYA K, OHSUNA T, INOUE A. Long-period hexagonal structures in melt-spun  $Mg_{97}Ln_2Zn_1$  (Ln=lanthanide metal) alloys [J]. Materials Transactions, 2003, 44: 2151–2156.
- [15] YAMASAKI M, ANAN T, YOSHIMOTO S, KAWAMURA Y. Mechanical properties of warm-extruded Mg-Zn-Gd alloy with coherent 14H long periodic stacking ordered structure precipitate [J]. Scripta Materialia, 2005, 53: 799–803.
- [16] YAMASAKI M, SASAKI M, NISHIJIMA M, HIRAGA K, KAWAMURA Y. Formation of 14H long period stacking ordered structure and profuse stacking faults in Mg-Zn-Gd alloys during

- isothermal aging at high temperature [J]. Acta Materialia, 2007, 55: 6798-6805.
- [17] KAWAMURA Y, YAMASAKI M. Formation and mechanical properties of Mg<sub>97</sub>Zn<sub>1</sub>RE<sub>2</sub> alloys with long-period stacking ordered structure [J]. Materials Transactions, 2007, 48: 2986–2992.
- [18] KAWAMURA Y, YOSHIMOTO S. High strength Mg-Zn-Y alloys with long period stacking structure [C]//Magnesium Technology 2005. Warrendale, PA: TMS, 2005: 499-502.
- [19] ONO A, ABE E, ITOI T, HIROHASHI M, YAMASAKI M, KAWAMURA Y. Microstructure evolutions of rapidly-solidified and conventionally-cast Mg<sub>97</sub>Zn<sub>1</sub>Y<sub>2</sub> alloys [J]. Materials Transactions, 2008 49: 990–994
- [20] KRESSE G, FURTHMÜLLER J. Efficiency of ab-initio total energy calculations for metals and semiconductors using a plane-wave basis set [J]. Computational Materials Science, 1996, 6: 15–50.
- [21] KRESSE G, FURTHMÜLLER J. Efficient iterative schemes for ab initio total-energy calculations using a plane-wave basis set [J]. Physical Review B, 1996, 54: 11169–11186.
- [22] PERDEW J P, BURKE K, ERNZERHOF M. Generalized gradient approximation made simple [J]. Physical Review Letters, 1996, 77: 3865-3868
- [23] MONKHORST H J, PACK J D. Special points for Brillouin-zone integrations [J]. Physical Review B, 1976, 13: 5188–5192.
- [24] BLÖCHL P E, JEPSEN O, ANDERSEN O K. Improved tetrahedron method for Brillouin-zone integrations [J]. Physical Review B, 1994, 49: 16223–16233.
- [25] DATTA A, RAMAMURTY U, RANGANATHAN S, WAGHMARE

- U V. Crystal structures of a Mg-Zn-Y alloy: A first-principles study [J]. Computational Materials Science, 2006, 37: 69-73.
- [26] WANG Y F, WANG Z Z, YU N, ZENG X Q, DING W J, TANG B Y. Microstructure investigation of the 6H-type long-period stacking order phase in Mg<sub>97</sub>Y<sub>2</sub>Zn<sub>1</sub> alloy [J]. Scripta Materialia, 2008, 58: 807–810.
- [27] CHEN P, LI D L, YI J X, TANG B Y, PENG L M, DING W J. Microstructure and electronic characteristics of the 6H-type ABACAB LPSO structure in Mg<sub>97</sub>Zn<sub>1</sub>Y<sub>2</sub> alloy [J]. Journal of Alloys and Compounds, 2009, 485: 672–676.
- [28] ZHU Y M, WEYLAND M, MORTON A J, OH-ISHI K, HONO K, NIE J F. The building block of long-period structures in Mg-RE-Zn alloys [J]. Scripta Materialia, 2009, 60: 980–983.
- [29] NISHIJIMA M, HIRAGA K, YAMASAKI M, KAWAMURA Y. The structure of guinier-preston zones in an Mg-2 at% Gd-1 at% Zn alloy studied by transmission electron microscopy [J]. Materials Transactions, 2008, 49: 227–229.
- [30] SONG Y, GUO Z X, YANG R. Influence of selected alloying elements on the stability of magnesium dihydride for hydrogen storage applications: A first-principles investigation [J]. Physical Review B, 2004, 69: 094205.
- [31] SAHU B R. Electronic structure and bonding of ultralight LiMg [J]. Materials Science and Engineering B, 1997, 49: 74–78.
- [32] ZUBOV V I, TRETIAKOV N P, TEIXEIRA R J N, SANCHEZ O J F. Calculations of the thermal expansion, cohesive energy and thermodynamic stability of a van der Waals crystal-fullerene C<sub>60</sub> [J]. Physics Letters A, 1995, 194: 223–227.

# $Mg_{97}Y_2Zn_1$ 合金中 18R 型长周期有序相的微观结构

唐平英1、吴萌萌1、唐壁玉1,2、王继伟2、彭立明3、丁文江3

- 1. 广西大学 化学化工学院,南宁 530004; 2. 湘潭大学 材料与光电物理学院,湘潭 411105;
  - 3. 上海交通大学 材料科学与工程学院, 轻合金精密成型国家工程研究中心, 上海 200030

摘 要:通过第一性原理计算研究  $Mg_{97}Y_2Zn_1$ 合金中 18R 型长周期有序相(LPSO)的微观结构, 从理论上确定 Zn 和 Y 原子在 LPSO 相中的排列。结果表明:添加原子首先分布在 18R 型 LPSO 相两端的层错层,然后向内部的层错层延伸。计算结果与实验现象非常吻合。同时,也揭示了 18R 与其他 LPSO 相之间的微观结构关系;结合能和形成焓表明了 18R 型 LPSO 相的稳定性与 Y 和 Zn 原子含量之间的关系。计算得到的电子结构揭示了 18R 型 LPSO 相微观结构和稳定性潜在的机理。

关键词:  $Mg_{97}Y_2Zn_1$  合金; 18R 型 LPSO 相; 第一性原理; 微观结构; 电子结构

(Edited by LI Xiang-qun)